Proceedings of 2017 IEEE
International Conference on Mechatronics and Automation
August 6 - 9, Takamatsu, Japan

Kalman Filter-based Navigation System for the Amphibious Spherical Robot

Huiming Xing[1, 2], Shuxiang Guo[1, 2, 3*], Liwei Shi[1, 2, 3*], Shaowu Pan[1, 2], Yanlin He[1, 2], Kun Tang [1, 2], Shuxiang Su[1,2], Zhan Chen[1, 2]

[1] Key Laboratory of Convergence Medical Engineering System and Healthcare Technology, the Ministry of Industry and Information Technology, School of Life Science, Beijing Institute of Technology, No.5, Zhongguancun South Street, Haidian District, Beijing 100081, China

[2] Key Laboratory of Biomimetic Robots and Systems, Ministry of Education, Beijing Institute of Technology, No.5, Zhongguancun South Street, Haidian District, Beijing 100081, China

[3] Faculty of Engineering, Kagawa University, 2217-20 Hayashi-cho, Takamatsu, Kagawa, Japan

shiliwei@bit.edu.cn, tangkun@bit.edu.cn, guoshuxiang@bit.edu.cn

* Corresponding author

***Abstract* - Robust and performing navigation systems for Autonomous Underwater Vehicles (AUVs) play a discriminant role towards the success of complex underwater missions. This paper presents a new design and development of a low-cost INS (Inertial Navigation System) using Miro-Electro-Mechanical-System (MEMS) inertial sensor and the pressure sensor (PS). The intensive pre-processing and modeling MEMES sensor's primitive, noisy motion data are outline, these techniques transform the erroneous motion data into practical motion indicators illustrated in 3D position, 3D velocity and 3D orientation. INS acts as a dead reckoning device. The pressure sensor is used to detect the depth data of underwater Vehicles. The quality of the filtering algorithm for the estimation of the AUV navigation state strongly affects the performance of the overall system. In this paper, the authors present adapt the Kalman Filter (KF) approach. Experiments were conducted to improve the navigation system performance of the INS and PS installed on the Amphibious Spherical Robot III (ASR III) for motion and attitude estimation. Lastly the experiment results are evaluated and verified using the sensor data from the navigation system.**

Index Terms – Amphibious Spherical Robot; Inertial Measurement System; Kalman Filter; Pressure Senor

I. INTRODUCTION

In recent years, Autonomous Underwater Vehicles (AUVs) were widely used in many fields of application: they are employed for scientific purposes (e.g. sample collection, exploration and surveillance of archaeological sites), to complete industrial tasks at high depths (for instance they are exploited in the Oil & Gas industry) [1],[2], to carry out reconnaissance and patrolling missions in the military field, or even to conduct search and rescue duties.

Regardless of the kind of tasks, the development of accurate and robust navigation system for AUVs [3],[4] is essential to reach the high control performance. In particular, one of the main factors influencing the AUVs navigation accuracy is the algorithm used to estimate the vehicle motion. They are usually based on Kalman Filters (KF), Extended Kalman Filter (EKF), Unscented Kalman Filter (UKF) or Particle Filter (PF) and make use of simplified kinematic or dynamic vehicle models.

Furthermore， different sets of sensors are employed during the underwater robot navigation. They may include, for instance, Inertial Measurement Units (IMU), or Fiber Optic Gyros (FOG) to measure underwater robot orientation, Pressure Sensors (PS) for depth measurements, Doppler Velocity Logs (DVL) [5],[6] to measure the vehicle translational velocity, acoustic localization systems [7] based on range measurements or on Ultra-Short BaseLine (USBL) [8]. Those sensors are mainly applied to the large AUV, and can assist the AUVs to have a robust and performing navigation systems. However, for some small underwater robots [9]-[11] including amphibious spherical robot, sensors, such as FOG, DVL, and USBL are too larger, heavier, and more difficult to be fixed on the robots. Therefore, we proposed a new Kalman filter-based navigation system employing IMU and the PS for the ASR-III.

The rest of paper is organized as follows. In section II, the novel amphibious spherical robot, also with its control method and some sensors mounted on it are introduced. In section III, the outline of the Kalman filter-based navigation system is presented. The navigation experiment with IMU and the pressure sensor is described in Section IV. And the conclusion and future work are presented in Section V.

II. AMPHIBIOUS SPHERICAL UNDERWATER ROBOT

A. *The Design of Robot*

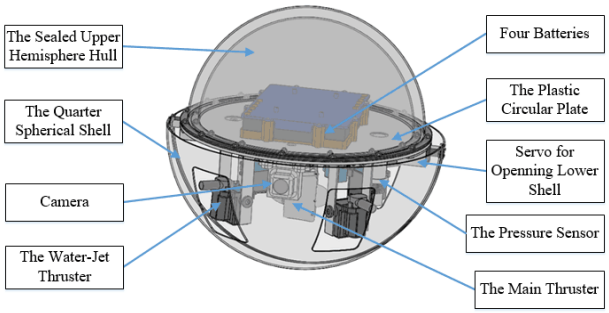

Fig.1 The overview structure of the ASR-III

The ASR-III (Amphibious Spherical Robot III) mainly consists of a sealed upper hemisphere hull, a plastic circular plate, four actuating units, a main thruster and sensors, such as the pressure sensor, IMU, cameras. The overview structure diagram of the robot is shown as Fig. 1. Four actuating units are symmetrical installed on the plastic circular plate. The control circuits, sensors and batteries are installed inside the sealed upper hemisphere hull in order to achieve the waterproof effect. As shown in Fig. 2 (a), each actuating unit includes two servo motors, a water-jet thruster. Fig. 2 (b) shows the mechanical structure of main thruster and Fig.2 (c) is the prototype of main thruster.

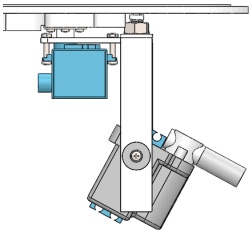

(a)

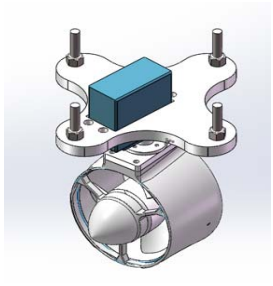

(b)

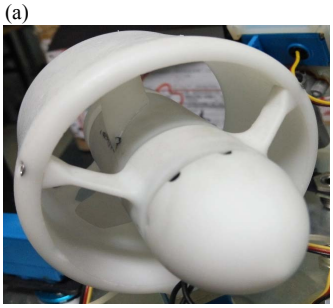

(c)

Fig.2 The actuating system (a. one actuating unit of mechanical leg, b. the mechanical structure of main thruster, c. the prototype of main thruster)

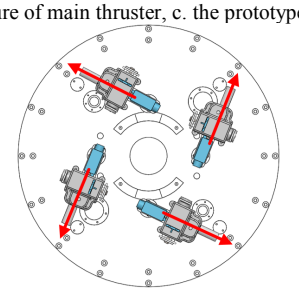

(a) Rotation movement with zero radius

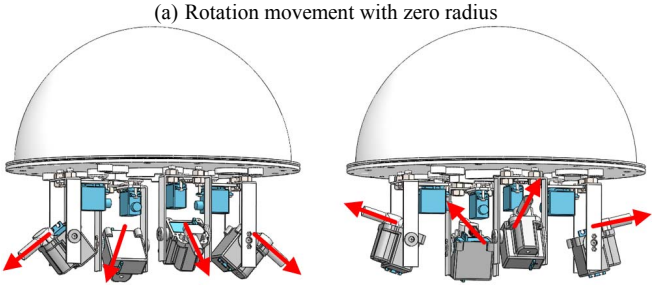

(b) Diving movement (c) Floating movement

Fig.3 The underwater movement of the ASR-III (the red arrow shows the direction of the water-jet force)

B. *The Propulsion System*

In the past of the research on the amphibious spherical robot [13]-[17], the on-land and underwater locomotion mainly rely on the four water-jet thrusters [12], but the velocity of the robot is very small and it need a more power thruster. In my research, I added a propeller thruster under the middle bottom board and it can implement exploration in wide-area environment. The main propeller thruster is shown as Fig.3. It can rotate in the horizontal plane, and the propeller thruster can realize the high-velocity motion after adjusting the orientation.

The four water-jet thrusters help the ASR-III realize the rotation movement with zero radius, sinking and floating movement as shown in Fig. 3. Fig.3 (a) shows the distribution of four water-jet thrusters to realize the rotation movement with zero radius. Fig.3 (b) and Fig.3 (c) indicate the vertical movement, sinking and floating respectively.

C. *The Sensors*

The ASR-III carries multiple sensors for the navigation system. Fig.4 shows IMU (ADSI16365), and PS.

Hereafter, the measurement equations modelling the sensor behavior will derived by taking into account the main features of the employed sensors and the main noise sources affecting the measurements:

(1) Robot depth η_{1z} measured by the depth sensor:

$$\eta_{1z}^{m} = \eta_{1z} + \delta_{1z} \tag{3}$$

where η_{1z}^{m} and η_{1z} are the measured and the true depths and δ_{1z} are the measurement noises.

(2) Robot orientations η_2 provided by IMU ADSI16365 (including 3D gyroscope, 3D accelerometer) through the attitude estimation filter starting from the following measures:

Robot angular velocity v_2 measured by the 3D gyroscope:

$$v_2^{m} = v_2 + \delta_{v2} \tag{4}$$

where v_2^{m} and v_2 denote the measured and the true angular velocities and δ_{v2} is the measurement noise;

Robot linear acceleration measured by the 3D accelerometer:

$$a_2^{m} = a_2 + \delta_a \tag{5}$$

where a_2^{m} and a denote the measured and true linear accelerations and δ_a is the measurement noise;

By suitably processing the above measurements, the attitude estimation filter is able to estimate the robot orientation η_2 that will be used in the subsequent developments of this paper as a visual measurement η_2^{m} modelled as:

$$\eta_2^{m} = \eta_2 + \delta_{2\eta} \tag{6}$$

where $\delta_{2\eta}$ is a further measurement noises.

Introducing the measurement vector $z = ((\eta_1^{m})^{T}, (\eta_2^{m})^{T})^{T}$, the measurement equations can be summarized as follows:

$$z = f(x) + v \tag{7}$$

$$f(x) = \left(\begin{array}{cc|cc} O_{3\times3} & O_{3\times3} & I_{3\times3} & O_{3\times3} \\ O_{3\times3} & O_{3\times3} & O_{3\times3} & I_{3\times3} \end{array}\right) x \tag{8}$$

$$\delta_{1\eta} = (\delta_{1x} \quad \delta_{1y} \quad \delta_{1z})^T \tag{9}$$

$$v = (\delta_{1\eta}{}^T \quad \delta_{2\eta}{}^T) = (\delta_{1x} \quad \delta_{1y} \quad \delta_{1z} \quad \delta_{2\eta}{}^T) \tag{10}$$

D. *The Control System of the ASR-III*

The robot control system of Amphibious Spherical Robot in Underwater is based on a traditional PID approach which is working on all the controlled DOFs of the robot (longitudinal, lateral and vertical translations and yaw rotations)

$$u(t) = K_p[e(t) + \frac{1}{T_i}\int_0^t e(t)dt + T_d\frac{de(t)}{dt}] \tag{11}$$

$$= K_p e(t) + K_i\int_0^t e(t)dt + K_d\frac{de(t)}{dt}$$

$$e(t) = x(t) - y(t) \tag{12}$$

where K_p, K_i, K_d are suitable (proportional, integral, derivative) gain matrices to be properly tuned so as to achieve the required control performance, $e(t)$ is the control error on all the robot DOFs(i. e. the difference between the desired value and the actual value) at time t, T_i and T_d are the time constant matrix of integration and derivative, $u(t)$ are the desired control force working on the robot (to be achieved through suitable control signals $x(t)$ of the robot motors, that is the motor rotation speed).

(a) IMU (b) Pressure sensor

Fig.4 The Sensors carried on the ASR-III

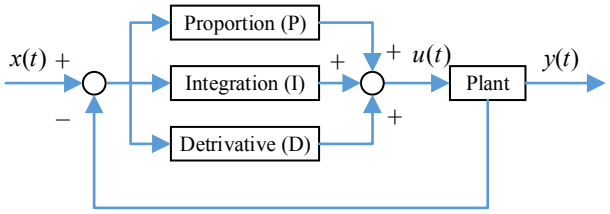

Fig.5 Block diagram of PID algorithm

III. Navigation System

As Section I mentioned, the ASR-III allows to easily and effectively test the performance of different navigation algorithms. The typical test architecture is schematized in Fig. 6.

A. *Kalman Filter*

Many researchers study to solve estimation problem of states variables about the dynamic system. The method based on theory of probability is configured probability space consisting of state variables. It is based on the estimate about state variable using system's dynamic characteristics and the measurement value. Typically based on Bayesian estimation technique, Kalman filter (KF), a particle filter and so forth have been actively studied in the field of localization.

$$\hat{x}_k^- = A\hat{x}_{k-1} + Bu_k \tag{13}$$

$$P_k^- = AP_{k-1}A^T + Q \tag{14}$$

In the system equation (1) (2), $\hat{x}_k^-$ is the state variable that want to optimize as the Kalman filter, A is the transform coefficients that connected between the previous step and the next step, B and u_k are the additional input value regardless of the system. P is the error covariance value, so it can be obtained by the system error Q and covariance value in the previous step. In the Kalman filter, Q is the most important element with the R of the observation equation.

$$K_k = P_k^- H^T(HP_k^- H^T + R)^{-1} \tag{15}$$

$$\hat{x}_k = \hat{x}_k^- + K_k(z_k - H\hat{x}_k^-) \tag{16}$$

$$P_k = P_k^- - K_k HP_k^- \tag{17}$$

In the observation equation (3) (4) (5), Kalman gain K_k is obtained by the error covariance P and the observation error R. Through the obtained Kalman gain previously, state variable values can be determined by predicted state variable values. This process not end instead of a single calculation and P values of the current state are readjusted by the Kalman gain, affect to the next step.

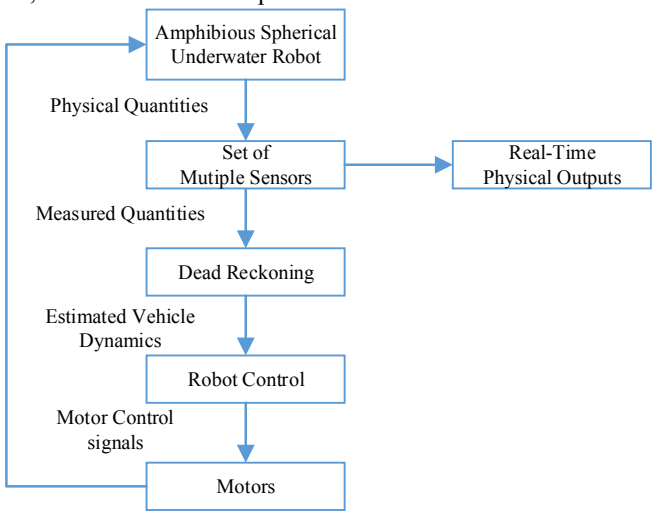

Fig.6 Online testing of navigation systems

B. *Dead Reckoning*

Navigation algorithm of INS consists of translation part and rotation part. The translation part is to conduct the integral of acceleration into velocity and translation of the ASR-III.

Given the velocity of the initial time t_0 as $v_{pd}(t_0)$, then we can get the velocity of the time t by the integration of the acceleration a_{pd}.

$$v_{pd}(t) = v_{pd}(t_0) + \int_{t_0}^t a_{pd}(t')dt' \tag{18}$$

Similarly, Given the position at the initial time t_0 as $r_{pd}(t_0)$, then the position at time t can be get via the integration of the velocity.

$$r_{pd}(t) = r_{pd}(t_0) + \int_{t_0}^{t} v_{pd}(t')dt' \\ = r_{pd}(t_0) + (t - t_0)v_{pd}(t_0) + \int_{t_0}^{t}\int_{t_0}^{t'} a_{pd}(t'')dt''dt' \quad (19)$$

Given the heading at the initial time t_0 as $\psi_{pd}(t_0)$, then the heading at time t can be get via the integration of the angular rate $\psi^b_{pd,z}$.

$$\psi_{pd}(t) = \psi_{pd}(t_0) + \int_{t_0}^{t} \psi^b_{pd,z}(t')dt' \quad (20)$$

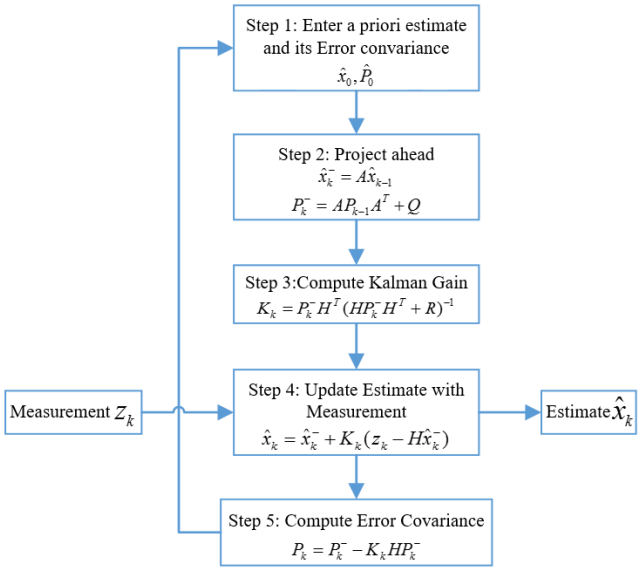

Fig.7 Algorithm of Kalman Filter

IV. Experimental Results

This section outlines the experimental results generated from the navigation system of the ASR-III with the IMU and the pressure sensor installed. In order to realize the navigation system, firstly, we evaluate our actuating system of the ASR-III and then take the heading control. Those experiments were conducted in an indoor pool of our laboratory, the size of which is 3m*2m*1m(height*width*depth), and the water is static without disturbances.

A. Thruster Force Testing and Evaluation

In our propulsion system, we have two types of thrusters. The type in Fig.2 (a) has low horsepower, and can not be used in wider area exploration. However, the resistance of rotation motion with zero radius is pretty slight because of the special spherical structure. Therefore, we use it to realize rotation control. And its force testing has been researched. There is no need to research on it. The other type showed in Fig.2 (c) has strong horsepower, and can move with large velocity. Here we test the characteristics of the main thruster by the simple device showed in Fig.8. After force analysis of the main thruster, we get the relationship between PWM signals and the thrust force by the equation (21).

$$F = mg\sin\theta \quad (21)$$

Fig. 9 shows that the force changes with the PWM signals (9%~13%), which is approximately linear. Therefore, the performance of the thruster is verified.

B. Navigation System Experiment

To evaluate the navigation system for the ASR-III, we carried out the experiment which the robot moves on a rectangle about 1.5m*2m. Fig.11 shows a video sequence of the horizontal underwater motion without disturbances and the depth value is about 15cm. In the experiment, we changed the heading angle, 0°, 90°, 180°, 270° at each turning point.

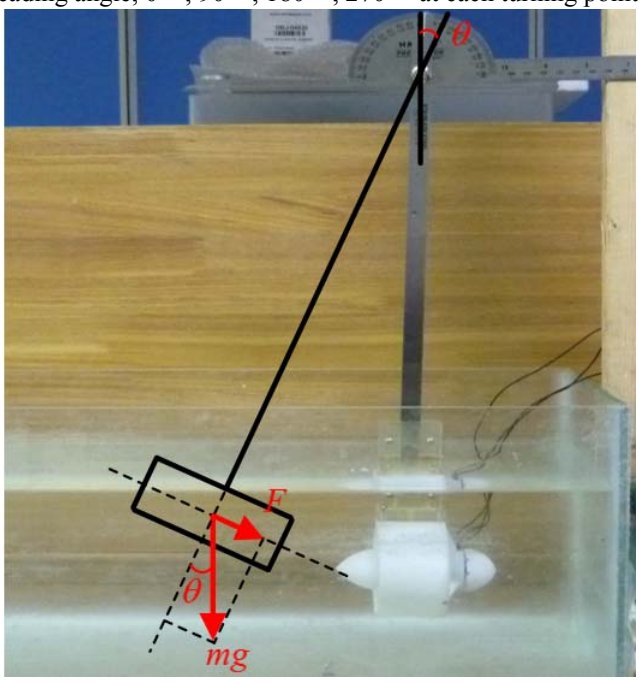

Fig. 8 The experimental device of main thruster

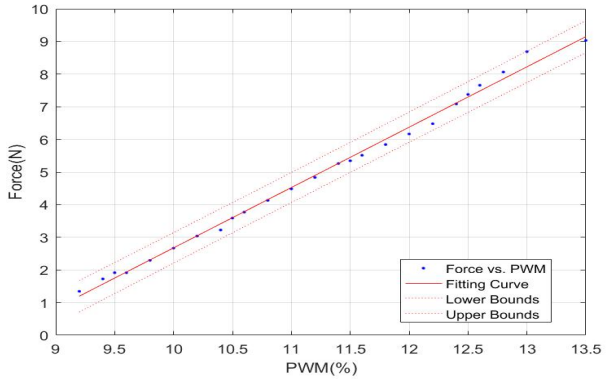

Fig.9 The results of main thruster testing

In our navigation system, we get the 3D position by the IMU and the pressure sensor and inertial data and depth data are measured with 200Hz. The depth data also can be computed by the IMU, but as we all know, it can generate cumulative error, and the error will become larger and larger over time, so we get the depth value by the pressure sensor. Fig.10 shows the green curve of the depth data measured with the pressure sensor and the red curve of the data predicted by Kalman filter. We can see that Kalman filter can estimate and re and correct systematic errors accurately. And the Kalman filter curve is much smoother.

Fig. 11 and Fig.12 show angle rate and acceleration measured with IMU and processed after Kalman filter. And

the curve after Kalman filter is smoother and Kalman filter will reduce measurement error, especially in Fig. 12 (the acceleration data).

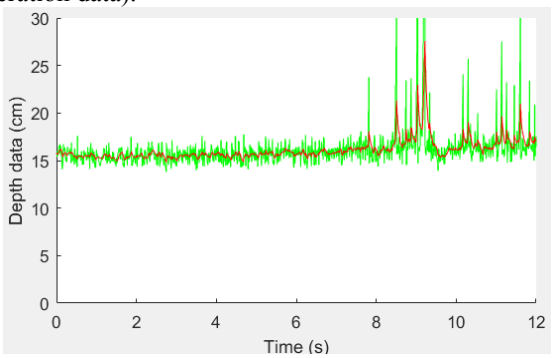

Fig.10 Depth data experiment (the green curve is measured with the pressure sensor; the red curve is predicted by Kalman filter)

Fig. 13 is the snapshots of our video about our navigation system experiment. We set the trajectory as a rectangle. And Our robot will last about 10s once on the rectangle (1.5m*2m). Fig. 14 and Fig.15 show the attitude and trajectory obtained by the ASR-III on the rectangle in the lab pool, so the ASR-III will turn three times, and the angle is 0° , 90° , 180° , 270° in Fig.14. The length of the rectangle trajectory is about 7m totally. As we can see, in Fig. 15, the accumulation error become larger over time.

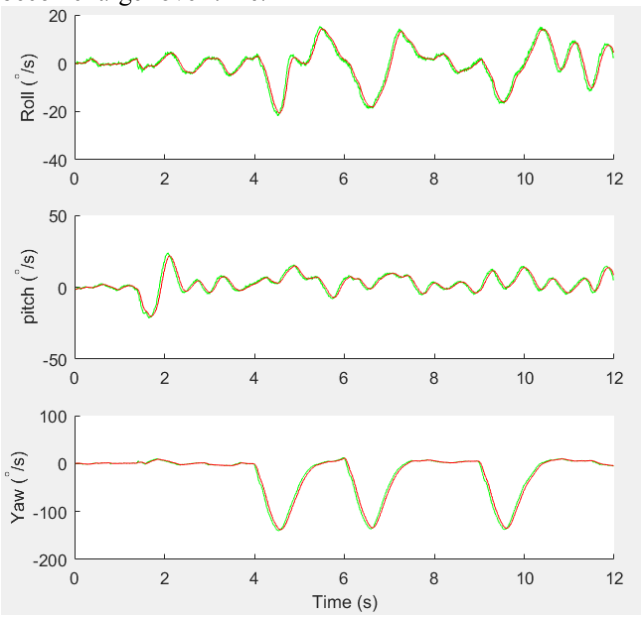

Fig.11 Angle rate of IMU (The green line is the measured data, and the red line is predicted by Kalman filter)

V. Conclusion and Future Work

This paper presents a new low cost integrated navigation system using MEMS, inertial sensor and the pressure sensor for the ASR-III. Firstly, we designed the ASR-III including a waterproof hull, an electrical system and a navigation system. And then we proposed a Kalman filter-based navigation system for the ASR-III. Finally, we conducted the experiments in a pool of our laboratory, and the results verified the accuracy of the navigation system. In the future, we will focus on the accuracy of the navigation system of the ASR-III via advanced methods based on Bayesian estimation technique, such as UKF, EKF and a particle filter. And for outdoor experiment, we will extend the navigation system by GPS (during periodic resurfacing), which will help the ASR-III realize the wider area navigation system.

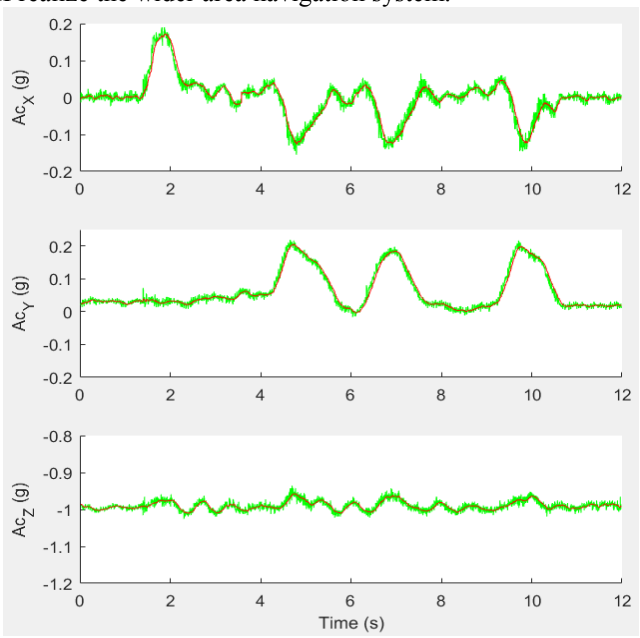

Fig.12 Acceleration of IMU (the green line is the measured data, and the red line is predicted by Kalman filter)

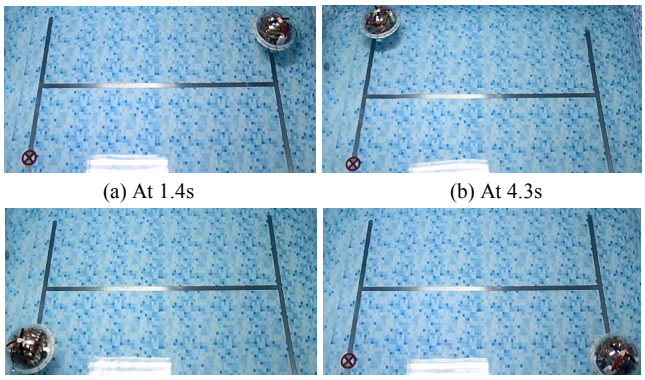

(a) At 1.4s (b) At 4.3s

(c) At 6.5s (d) At 8.2s

Fig.13 Screenshots of our navigation experiment

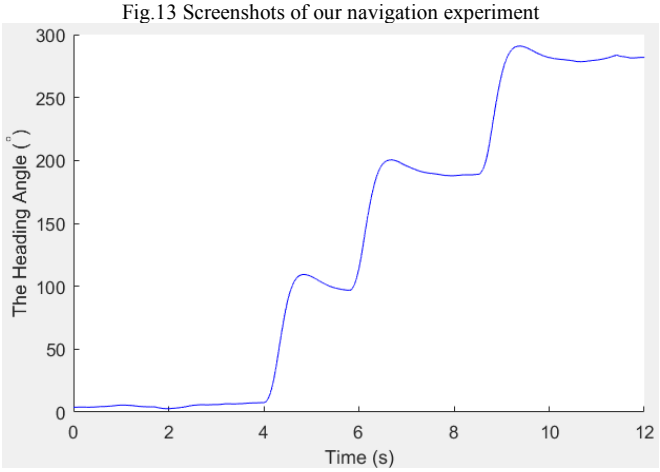

Fig.14 Attitude of ASR-III

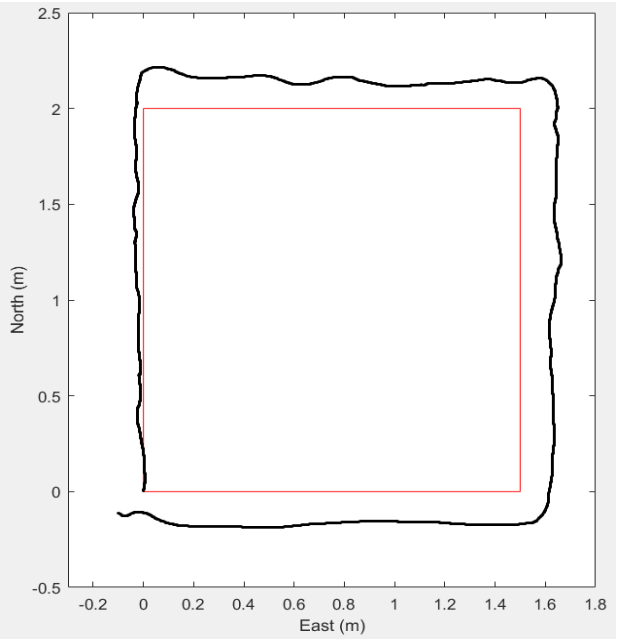

Fig.15 Position trajectory of IMU (The red rectangle is measured by ruler, and the black line presents trajectory after Kalman filter)

ACKNOWLEDGMENT

This work was supported by National Natural Science Foundation of China (61503028, 61375094), and Excellent Young Scholars Research Fund of Beijing Institute of Technology (2014YG1611). This research project was also partly supported by National High Tech. Research and Development Program of China (No.2015AA043202).

REFERENCES

[1] E. Cavallo, R. Michelini, V. Filaretov, "Conceptual design of an AUV equipped with a three degrees of freedom vectored thruster", *Journal of Intelligent Robotic Systems*, vol. 39, no.4, pp. 365–391, 2004.

[2] Liwei. Shi, Rui. Xiao, Shuxiang. Guo, et al. "An attitude estimation system for amphibious spherical robots", *Proceedings of IEEE International Conference on Mechatronics and Automation*, pp. 2076-2081, 2015.

[3] Sheijani, Mohammad Shabani, "Implementation and performance comparison of indirect Kalman filtering approaches for AUV integrated navigation system using low cost IMU", *Proceeding of IEEE Iranian Conference on Electrical Engineering*, pp. 1-6, 2013.

[4] Yuan, DY, Ma, XC, et al. "Dynamic initial coarse alignment of SINS for AUV using the velocity loci and pressure sensor". *IET Science Measurement and Technology*, vol. 10, no. 8, pp. 926-933, 2016.

[5] Tal, Asaf; Klein, Itzik; Katz, Reuven, "Inertial Navigation System/Doppler Velocity Log (INS/DVL) Fusion with Partial DVL Measurements", *Sensors*, vol. 17, no. 2, 2017.

[6] Li W, Zhang L, Sun F, et al. "Alignment calibration of IMU and Doppler sensors for precision INS/DVL integrated navigation", *International Journal for Light and Electron Optics*, vol. 23, no. 126, pp. 3872-3876, 2015.

[7] Xiao G, Wang B, Deng Z, et al. "An Acoustic Communication Time Delays Compensation Method for Master-Slave AUV Cooperative Navigation". *IEEE Sensors Journal*, vol. 17, no. 2, pp. 504-513, 2016.

[8] Morgado M, Batista P, Oliveira P, et al. "Position USBL/DVL sensor-based navigation filter in the presence of unknown ocean currents", *Decision and Control,* vol. 12, no. 47, pp. 2192-2197, 2011.

[9] L. Shi, S. Guo, and K. Asaka, "Development of a New Jellyfish-type Underwater Microrobot", *International Journal of Robotics and Automation*, vol. 26, no.2, pp. 229-241, 2011.

[10] A. Villanueva, C. Smith, and S. Priya, "A biomimetic robotic jellyfish (Robojelly) actuated by shape memory alloy composite actuators", *Bioinspiration & Biomimetics*, vol. 6, no. 3, 036004, pp.1-16, 2011.

[11] L. Shi, S. Guo, S. Mao, M. Li, and K. Asaka, "Development of a Lobster-inspired Underwater Microrobot", *International Journal of Advanced Robotic Systems*, vol. 1, no. 10, pp. 1-15, 2013.

[12] X. Lin, S. Guo, "Development of a Spherical Underwater Robot Equipped with Multiple Vectored Water-Jet-Based Thrusters", *Journal of Intelligent and Robotic Systems*, vol. 67, no. 3, pp. 307-321, 2012.

[13] Yaxin Li, Shuxiang Guo, Yu Wang, "Design and characteristics evaluation of a novel spherical underwater robot", *Robotics and Autonomous Systems*, DOI: 10.1016/j.robot.2017.03.014, 2017.

[14] Shuxiang Guo, Yanlin He, Liwei Shi, Shaowu Pan, Kun Tang, Rui Xiao, Ping Guo, "Modal and fatigue analysis of critical components of an amphibious spherical robot", *Microsystem Technologies*, DOI:10.1007/s00542-016-3083-0, 2016.

[15] Maoxun Li, Shuxiang Guo, Hideyuki Hirata, Hidenori Ishihara, "A Roller-skating/Walking Mode-based Amphibious Robot", *Robotics and Computer Integrated Manufacturing*, vol. 44, pp.17-29, 2016.

[16] Jian Guo, Shuxiang Guo, Liguo Li, "Design and Characteristic Evaluation of a Novel Amphibious Spherical Robot", *Microsystem Technologies*, DOI: 10.1007/s00542-016-2961-9, 2016.

[17] Maoxun Li, Shuxiang Guo, Jin Guo, Hideyuki Hirata, Hidenori Ishihara, "Development of a biomimetic underwater microrobot for a father‐ son robot system", *Microsystem Technologies*, vol. 23, no. 4, pp.849-861, 2016.

[18] Yanlin He, Shuxiang Guo, Liwei Shi, "Preliminary Mechanical Analysis of an Improved Amphibious Spherical Father Robot", *Microsystem Technologies*, DOI 10.1007/s00542-015-2504-9, 2015.

[19] Chunfeng Yue, Shuxiang Guo, Liwei Shi, "Design and Performance Evaluation of a Biomimetic Microrobot for the Father-son Underwater Intervention Robotic System", *Microsystem Technologies*, DOI: 10.1007/s00542-015-2457-z, 2015.

[20] Chunfeng Yue, Shuxiang Guo, Maoxun Li, Yaxin Li, Hideyuki Hirata, Hidenori Ishihara, "Mechantronic System and Experiments of a Spherical Underwater Robot: SUR-II", *Journal of Intelligent and Robotic Systems*, DOI 10.1007/s10846-015-0177-3, vol. 80, no. 2, pp. 325-340, 2015.